TR-161

WATER AND SOLUTE FLOW IN A HIGHLY STRUCTURE SOIL

Willem J. Heuvelman

Kevin J. McInnes

Larry P. Wilding

C. Tom Hallmart

December 1993

TECHNICAL REPORT

WATER AND SOLUTE FLOW IN A HIGHLY-STRUCTURED SOIL

Project No. 02
(September 1, 1990 - August 31, 1992)
Grant Numbers
14-08-001-G1592
14-08-001-G2048

by

Willem J. Heuvelman
Graduate Research Assistant

Kevin J. McInnes
Assistant Professor
Department of Soil and Crop Science
Texas A&M University
College Station, Texas

Larry P. Wilding
Professor
Department of Soil and Crop Science
Texas A&M University
College Station, Texas

C. Tom Hallmark
Professor
Department of Soil and Crop Science
Texas A&M University
College Station, Texas

Technical Report No. 161
Texas Water Resources Institute
The Texas A&M University System
College Station, Texas 77843-2118

December 1993

The research on which this report is based was financed in part by the United States Department of the Interior, Geological Survey, through the Texas Water Resources Institute.

DISCLAIMER

Contents of this publication do not necessarily reflect the views and policies of the United States Department of the Interior, nor does mention of trade names or commercial products constitute their endorsement by the United States Government.

All programs and information of the Texas Water Resources Institute are available to everyone without regard to race, ethnic origin, religion, sex, or age.

ACKNOWLEDGEMENTS

The financial support of the Texas Water Resources Institute is gratefully acknowledged.

Texas A&M students Joe Pat Wallace, Rica Muhl and Nazrul Chowdhury contributed to the success of this research. Special thanks go to June E. Wolfe III for his stimulating ideas and technical assistance.

ABSTRACT

Prevention of groundwater contamination by agricultural activities is a high priority in the United States. Water and contaminants often follow particular flow paths through the soil that lead to rapid movement of pesticides out of the rootzone. An improved understanding of why water and solute follow particular flow paths is needed to identify soils that allow agricultural chemicals to move rapidly to groundwater. The rate that water and contaminants are transferred from the soil surface to groundwater may be related to the degree of flow path channelization (convergence or divergence of water flow paths). This project was designed to test the feasibility of measuring the degree of channelization as water percolates through structured soils. A flow interceptor device consisting of 98 individual 25 by 25 mm cells operating under tension was constructed for this purpose.

Water flux probability density distributions (pdd's) were measured at 0.3, 0.6 and 0.9 m depth in Ships clay (very-fine, mixed, thermic, Chromic Udic Haplusterts). Water flux and solute travel time pdd's were measured at 0.3, 0.9 and 1.2 m in Silawa loamy fine sand (fine-loamy, siliceous, thermic, Ustic Haplustalfs). Both probability distributions were fitted with log-normal functions. In Ships clay, water flow paths converged as water moved from 0.3 to 0.9 m depth, while in Silawa loamy fine sand flow paths converged from 0.3 to 0.9 and diverged from 0.9 to 1.2 m depth. This convergence and divergence of water flux in the soil was related to changes in structural definition with depth. Convergence of water and solute flow is expected to increase the pollution potential of the

soil because of increased bypassing of soil matrix and increased pore water velocities.

Solute travel time pdd's for Silawa at 0.9 and 1.2 m depth were predicted with a stochastic transfer function model calibrated at 0.3 and 0.9 m depth, respectively, and compared to the actual measured travel time pdd's at 0.9 and 1.2 m. From this it was concluded that water flux measurements at the surface alone are, in general, not a suitable way to predict water and solute fluxes at lower depths.

Spatial variability of water fluxes and bromide fluxes were highly correlated, and the coefficient of variation of both depended on the horizon in which the measurements were taken.

PURPOSE OF RESEARCH

This project was designed to test the feasibility of measuring the convergence or divergence of water flow paths as water percolates through structured soil. Convergence or divergence of water flow paths influence the amount of soil matrix that is bypassed and consequently the travel time of a contaminant moving from the soil surface to groundwater. Possible retardation by sorption and degradation of contaminants is influenced by their travel time through the soil. Bypass flow increases the possibility of contaminants reaching groundwater because is decreases the time that they reside in the soil (Economy and Bowman, 1992).

TABLE OF CONTENTS

LIST OF FIGURES

page

LIST OF TABLES

INTRODUCTION

Prevention of groundwater contamination by agricultural activities is a high priority in the United States. Pesticide concentrations believed unsafe in water supplies have been established by the Environmental Protection Agency through "risk-based concentration limits" and "maximum contaminant levels." Allowable concentrations will likely become more stringent as analytical methods for measurement improve, more toxicology research becomes available, and public perceptions of risk intensify.

Detectable levels of pesticides can result when only a small fraction of chemicals that are applied escape the root zone and reach the groundwater. Pesticide management practices can be improved with better understanding and knowledge of the mechanisms and pathways by which contaminants reach groundwater. Likely pathways (flow paths) for rapid movement ("channeling" or "bypass flow") of pesticides out of the rootzone may result from the activity of soil organisms, or may be created by pedogenic processes that affect the soil structure. An improved understanding of why water and solutes follow particular flow paths is needed to identify soils through which agricultural chemicals might move rapidly to groundwater, and to improve existing agricultural management practices on these soil types.

The rate at which water is transferred from the soil surface to groundwater is related to the degree of channelization. Water velocity at a given flu increases as the fraction of the soil transmitting that flux decreases. This means that if the fraction of pore space transmitting water

decreases by a factor x, the relative water velocity increases by the same factor x, as shown in Fig. 1.

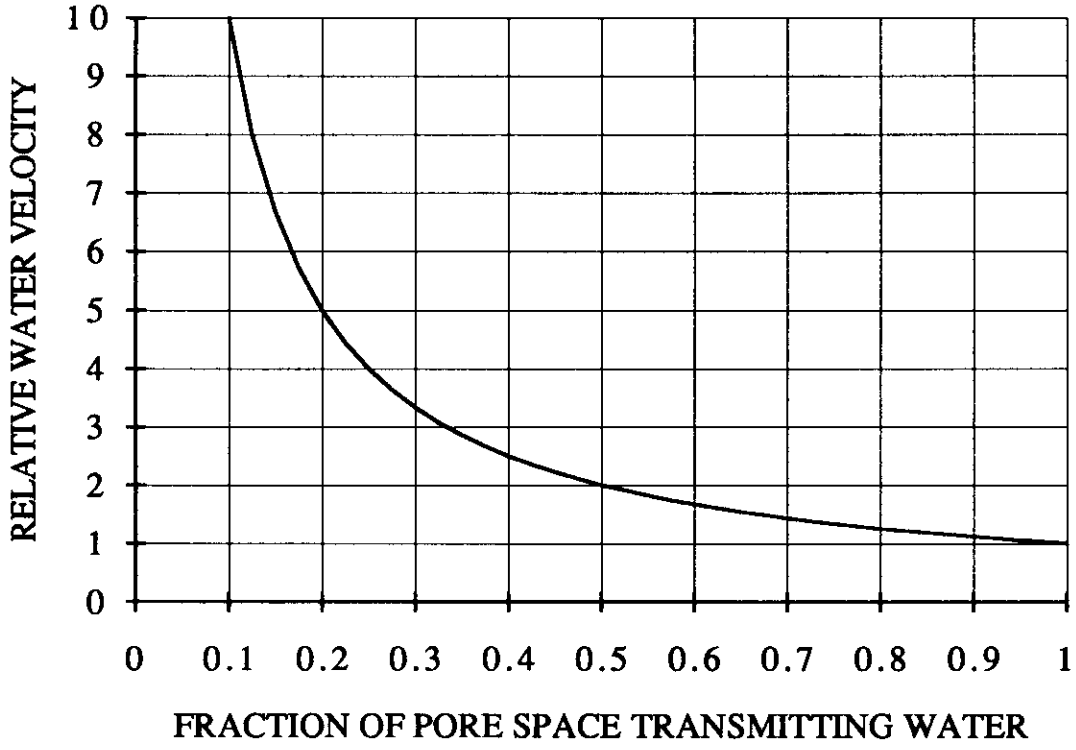

Figure 1. Influence of active pore space on water velocity.

When the fraction of pores transmitting water is small, the travel time for a given parcel of water from surface to groundwater is also small, due to the higher flow rate. Water-conducting pores in clayey soils sometimes occupy less than 1% of the total soil volume (Bouma, 1984). Therefore, traditional estimates of travel times based on water flowing through the total pore space may be grossly overestimated.

Travel times may be derived from (measured) water flux spatial probability density distributions (pdd's). The simplest case would arise if the water flux pdd was independent of depth. If the flux pdd varies with depth, the relationship is more complex. There is no known *a priori* method of determining the relationship between the two distributions.

The original objective of the project was to predict the dynamics of water and solute transfer in structured (fissured) soils, using a minimum dataset. The minimum dataset was to consist of a description of soil structure or soil morphological descriptions, plus measurements of water flow characteristics made at the soil surface. This can be done by linking the solute travel time with the spatial water flux pdd's in structured soils, and by predicting the spatial water flux pdd's from surface measurements and/or soil descriptions. The latter seems feasible since Coen and Wang (1989) found that hydraulic properties of some soils could be predicted from morphological observations and Shepard (1993) predicted hydraulic conductivity functions of some soils from soil water retention curves. Most of the work in this project, however, is concentrated on analyzing water and solute flow with depth and understanding how the soil structure at given depths affects flow rates.

MATERIALS AND METHODS

Sampler construction

Measurements of spatial water flux pdd's required development of a device consisting of a closely-spaced set of "flow interceptors," each designed to catch water and solute flow from the soil directly above. Individual interceptor cell bases were milled from a 25 mm square PVC bar. A porous stainless steel plate (21 mm square, 1 mm thick, and 5 μm pore diameter) was mounted at 2 mm from the top with stainless steel screws. To prevent air leakage, an O-ring was placed between the PVC base and the porous plate, within an imaginary square formed by the screws. A schematic is shown in Fig. 2.

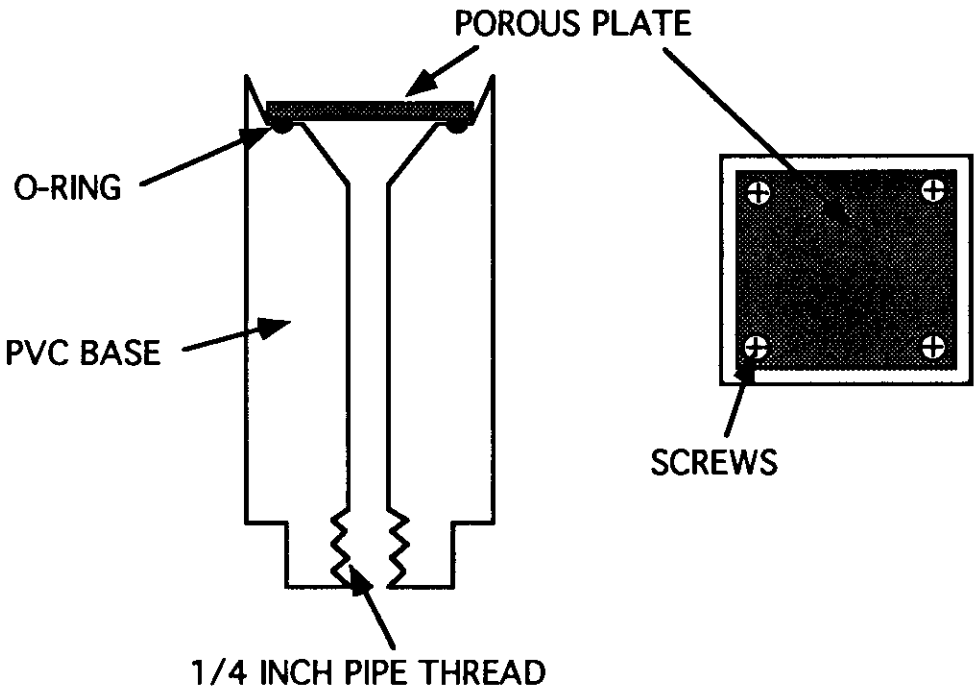

Figure 2. Individual interceptor cell as viewed from the side and top.

Individual interceptor cells were arranged in a 7 by 14 grid (98 individual samplers). Cells were connected with 0.125 mm (inner diameter) nylon tubing to individual 1 liter solution collection bottles, which were connected to a common vacuum system (Fig. 3). A manifold made of two 6 mm thick aluminum plates, with 12.5 mm thick ensolite foam (Hibco Plastics, Inc.) on the bottom to seal the system, was pressed on top of the collection bottles. Partial vacuum (-10 kPa) was applied to the bottles through the manifold system with vacuum pumps powered from deep-cycle marine batteries (12 volts DC). A water trap and desiccator were installed between the bottles and the vacuum system to prevent water from entering the vacuum pump and to measure evaporation from the bottles. This step was not needed since only very small amounts of water vapor were intercepted.

Field measurements

Two soils were studied, Ships clay (very-fine, mixed, thermic, Chromic Udic Haplusterts) and Silawa loamy fine sand (fine-loamy, siliceous, thermic, Ustic Haplustalfs). Nu-Mex Sahara bermudagrass was growing on both soils at the time of the experiments. Water was applied to the surface of the soils in a 1.2 by 1.2 m infiltration square and maintained at a constant depth of about 5 cm. Part of the downward water flux beneath the infiltration square was collected with the flow interceptor device (Fig. 4). Samples were collected 0.3, 0.6 and 0.9 m below the surface (not simultaneously but during independent experiments) for Ships clay, and at 0.3, 0.9 and 1.2 m for Silawa loamy fine sand. The measurements at 0.3 m in Silawa were done in the laboratory on a block of soil that was dug out of the field, because the tunnel collapsed during

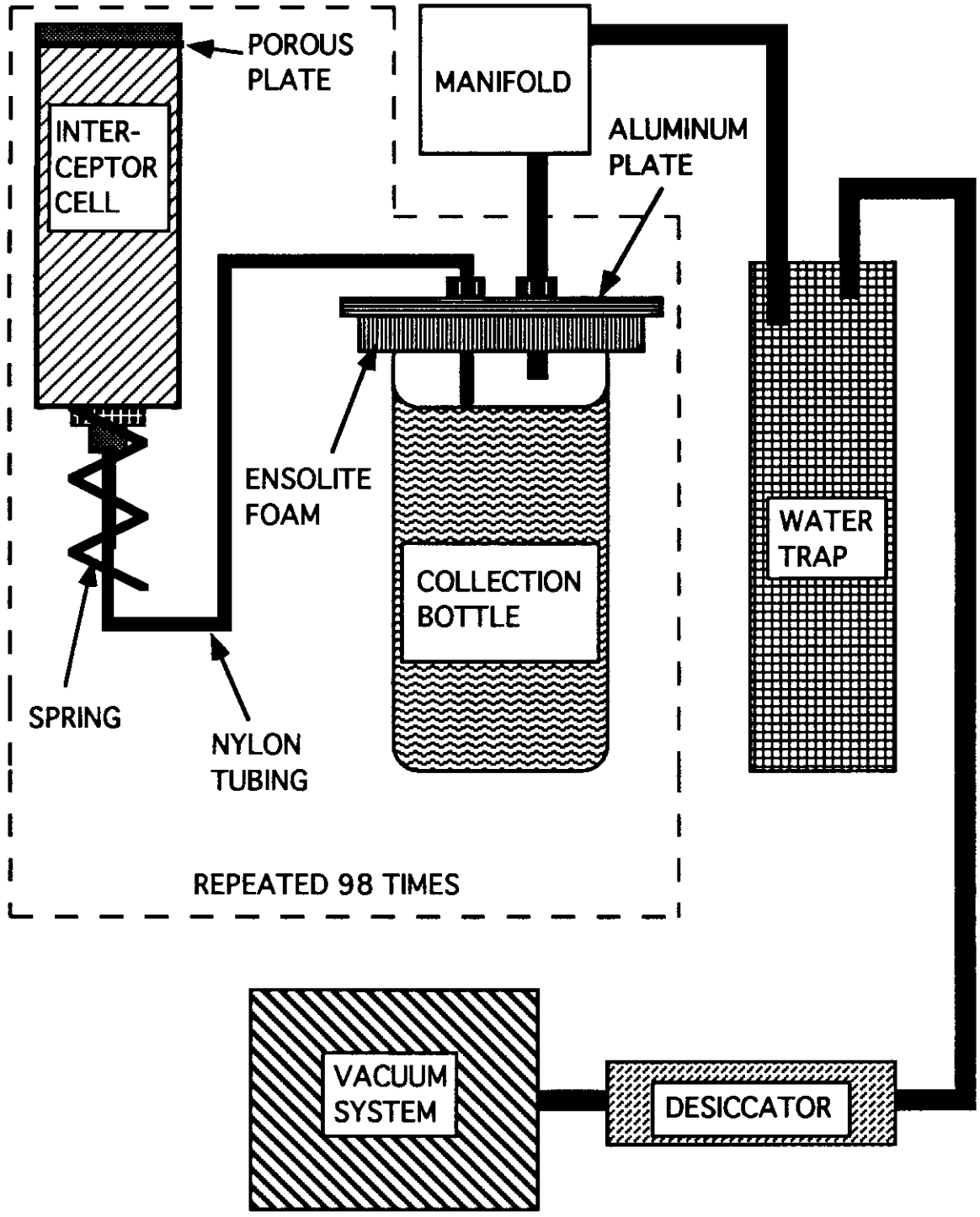

Figure 3. Flow interception and collection system.

attempted measurements in the field. This may have influenced measurements significantly. Water flux pdd's were determined for Ships clay while water flux and travel time pdd's were determined for Silawa loamy fine sand.

To install the interceptor device, a 2-m long tunnel was dug into a pit face. The first tunnel at each location was dug at the lowest measurement depth. From there, the tunnel was extended upward for the next set of measurements at the next depth, and then up to the third depth. The ceiling at the end of the tunnel was made as flat and level as possible using a knife. Care was taken not to smear the soil on the ceiling. Any residual roughness on the ceiling was smoothed with moist medium-fine sand. The interceptor cells were pushed up to the soil ceiling and held there with an air jack, which was made of two steel boxes, one fitting loosely over the other, with an inflatable tube in-between. Each cell was loaded on an individual spring (Fig. 3) to compensate for any unevenness of the soil ceiling and to ensure that each cell made good contact with the ceiling The infiltration square was pushed into the soil surface above the interception device after the vegetation (grass) was clipped and removed. One location was studied in the Ships clay (Ships) and two locations were studied in the Silawa loamy fine sand (Silawa1 and Silawa2). Six to nine solution samples were collected at 1 to 8 h intervals, depending on the soil horizon, with the first sample being plain water. The plain water was applied to saturate the soil and to create the correct boundary conditions for the solute transport model.

The solute tracer used in this study was bromide, applied as KBr solution. Bromide is conservative in terms of adsorption and decay. In order to avoid above-surface mixing, a pulse of bromide was applied to

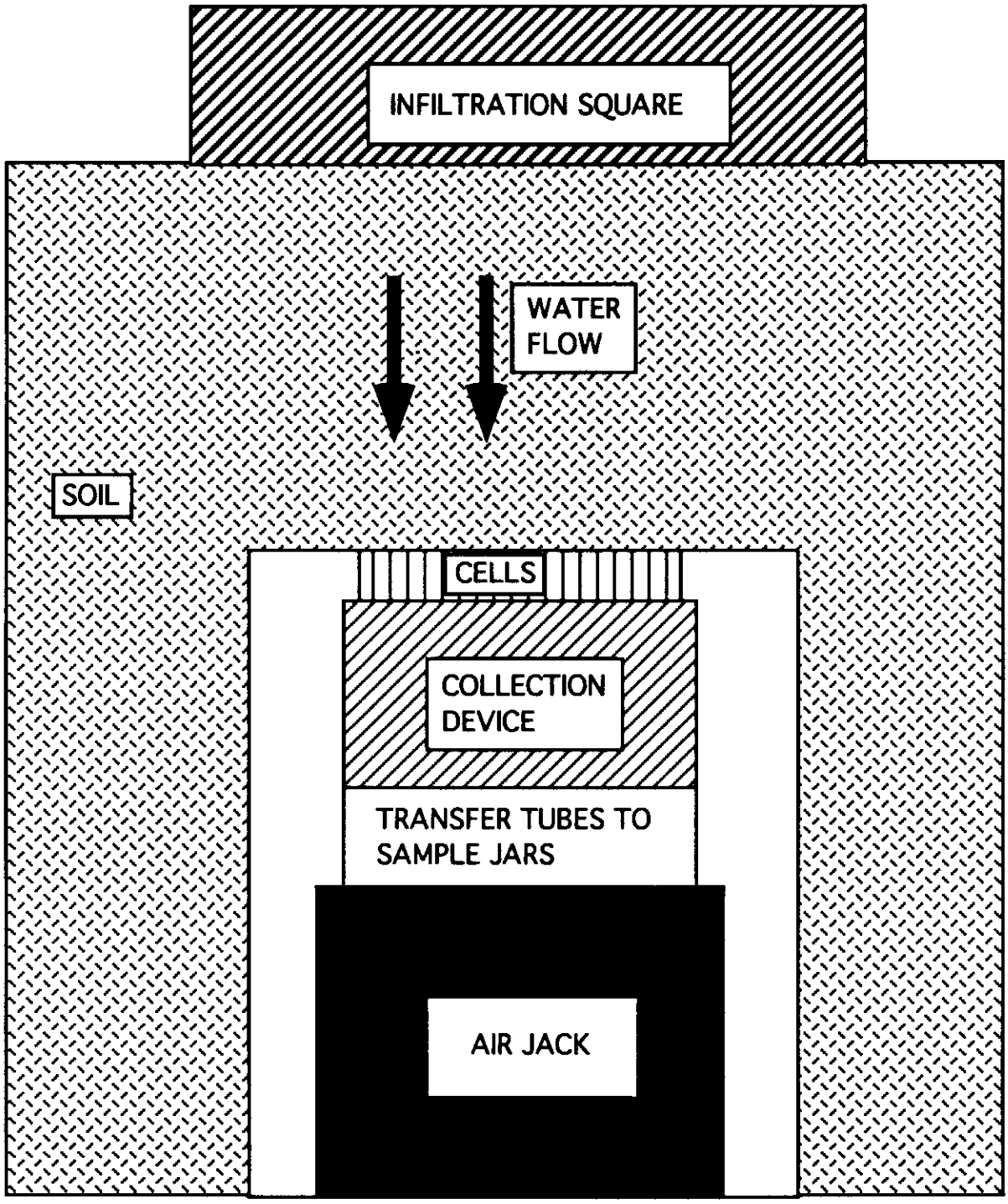

Figure 4. Installation scheme.

the infiltration square after the first sample was collected and after all plain water in the square had been allowed to infiltrate. Solution samples collected from the interceptor device were analyzed for bromide with an Orion model 94-35 bromide electrode and an Orion model 90-01 single junction reference electrode. Factory-recommended addition of ionic strength adjustor to the solution sample did not influence the electrode reading and this step was therefore needed.

Data analysis and modeling

In the data analysis, only the 60 (5 by 12) inner cells were considered. Measurements from the 38 outer cells were not used because these cells tended to exhibit a higher mean value and a different probability distribution of intercepted water fluxes than the inner cells. This convergence of water from the surrounding soil into the outer cells was expected at the time of design and construction of the interceptor. The water volume and bromide concentration of the intercepted solute flux of each solution sampler were used to calculate the travel time pdd's and the spatial relative flux (flux intercepted by one sampler divided by the sum of fluxes intercepted by all 60 samplers) pdd's.

The pdd of the time that it takes for a solute molecule to move from the soil surface to a depth z can be calculated directly from the measured intercepted water fluxes and corresponding bromide concentrations. Because infiltration and percolation rates may change with time and place, time was measured in terms of cumulative intercepted drainage (D) for more convenient comparison of travel time pdd's at different locations.

The empirical travel time pdd, exclusively based on data, is a stepwise linear function which mathematically can be expressed as

$$pdd(z,i) = \frac{c^i(z,\Delta D^i)\cdot\Delta D^i}{\sum_{i=1}^{n}[c^i(z,\Delta D^i)\cdot\Delta D^i]} \qquad (1)$$

where $c^i(z,\Delta D^i)$ is the concentration, ΔD^i is the intercepted drainage, and $c^i(z,\Delta D^i)\cdot\Delta D^i$ is the amount of bromide intercepted at depth z in the i^{th} interval, and $\sum_{i=1}^{n}[c(z,\Delta D^i)\cdot\Delta D^i]$ is the total amount of intercepted tracer at depth z, while n ranges from 5 to 8.

The empirical spatial relative flux pdd is simply a frequency distribution of the relative fluxes. Mathematically this can be expressed as

$$pdd(z,j) = \#\text{ of measurements in class j} \qquad (2)$$

or

$$pdd(z,j) = \frac{\#\text{ of measurements in class j}}{\#\text{ of all measurements (=60)}} \qquad (3)$$

Since it was known from literature that distributions of both travel time (White, 1987) and solute flux pdd's (Nielsen *et al.*,1973) are approximately log-normal, the cumulative distributions of travel time and relative fluxes were fitted with a log-normal cumulative distribution function (cdf). Cdf's can be converted into probability density functions (pdf's), and pdf's into cdf's by differentiation and integration, respectively:

$$f(D) = \frac{dF(D)}{dD} \quad \text{and} \quad F(D) = \int_0^D f(D')\ dD' \qquad (4)$$

where $F(D) = P(\text{Drainage} \leq D)$ is the cdf and f(D) is the pdf.

Transfer function models have been used for a long time in many fields. In hydrology for instance, the transfer function is used as the Instantaneous Unit Hydrograph and converses effective rainfall into drainage basin outflow. The general equation of the transfer function model, which also is known as convolution or Duhamel integral, is

$$Out(t) = \int_0^{t' \leq t_o} f(\tau)In(t-\tau)\, d\tau = \int_0^{t' \leq t_o} f(t-\tau)In(\tau)\, d\tau \qquad (5)$$

where $t' = t$ when $t' \leq t_o$ and $t' = t_o$ when $t > t_o$, $In(\tau)$ is the input function on the interval 0 to t_o and $f(t-\tau)$ is the kernel or transfer function (Chow, 1964). A stochastic-convective log-normal transfer function model approach was used to predict the travel time pdd at a lower depth L given the measured pdd at another depth $z < L$. This transfer function model does not assume any physical transport mechanisms, but uses linear superposition of travel time probabilities and mass balance (Jury and Flühler, 1992). It implies that the probability for a bromide molecule to reach a depth z in "time" less than or equal to D ("travel drainage") is equal to the probability that this same molecule reaches a depth L in "time" less than or equal to $\frac{L}{z} \cdot D$ (Jury and Roth, 1990), so

$$F(z,D) = F(L, \frac{L}{z} \cdot D) \qquad (6)$$

and by (4)

$$f(z,D) = \frac{L}{z} \cdot f(L, \frac{L}{z} \cdot D) \qquad (7)$$

This will only hold, of course, in a homogeneous profile and under steady state saturated flow conditions. The latter condition was satisfied in our experiments. From 6 or 7 that it follows that

$$E_L[D_L] = E_z[\frac{L}{z} \cdot D_z] = \frac{L}{z} \cdot E_z[D_z] \qquad (8)$$

and

$$Var_L[D_L] = Var_z[\frac{L}{z} \cdot D_z] = (\frac{L}{z})^2 \cdot Var_z[D_z] \qquad (9)$$

where $E_L[D_L]$ and $Var_L(D_L)$ are the mean (expected value) and the variance of the travel time ("travel drainage") to depth L.

The log-normal pdf (transfer function) can be expressed as

$$f(z,D_z) = \frac{1}{\sqrt{2\pi}\,\sigma_z D_z} \cdot \exp\left(\frac{-\{\ln(D_z)-\mu_z\}^2}{2\sigma_z^2}\right) \qquad (10)$$

where D_z is the cumulative drainage, μ_z and σ_z^2 are the mean and the variance of the log-transformed data at depth z. It follows from (8) and (9) that

$$\mu_L = E_z[\ln(\frac{L}{z} \cdot D_z)] = E_z[\ln(D_z) + \ln(\frac{L}{z})] = \mu_z + \ln(\frac{L}{z}) \qquad (11)$$

and

$$\sigma_L^2 = Var_z[\ln(\frac{L}{z} \cdot D_z)] = Var_z[\ln(D_z) + \ln(\frac{L}{z})] = \sigma_z^2 \qquad (12)$$

This means that by transformation of the mean and the variance, the log-normal travel time pdf at depth z (10) can be used to predict the travel time pdf at depth L

$$f(L,D_L) = \frac{1}{\sqrt{2\pi}\,\sigma_z D_L} \cdot \exp\left(\frac{-\{\ \ln(D_L) - [\mu_z + \ln(\frac{L}{z})]\ \}^2}{2\sigma_z^2} \right) \qquad (13)$$

where now μ_z and σ_z^2 are known from calibration at depth z.

RESULTS

Spatial analysis of water and bromide fluxes

The intercepted water fluxes in both the Ships and Silawa soils showed considerable spatial variability. The degree of spatial variability strongly depended on the depth at and the horizon in which the measurements were taken, as can be seen from the differences in the coefficients of variation (CV) of the various samples (Fig. 5). The sandy top layer of Silawa1 and Silawa2 showed the least amount of spatial variability in water fluxes while Silawa1 and Ships expressed the highest amounts of variation at 0.9 m depth.

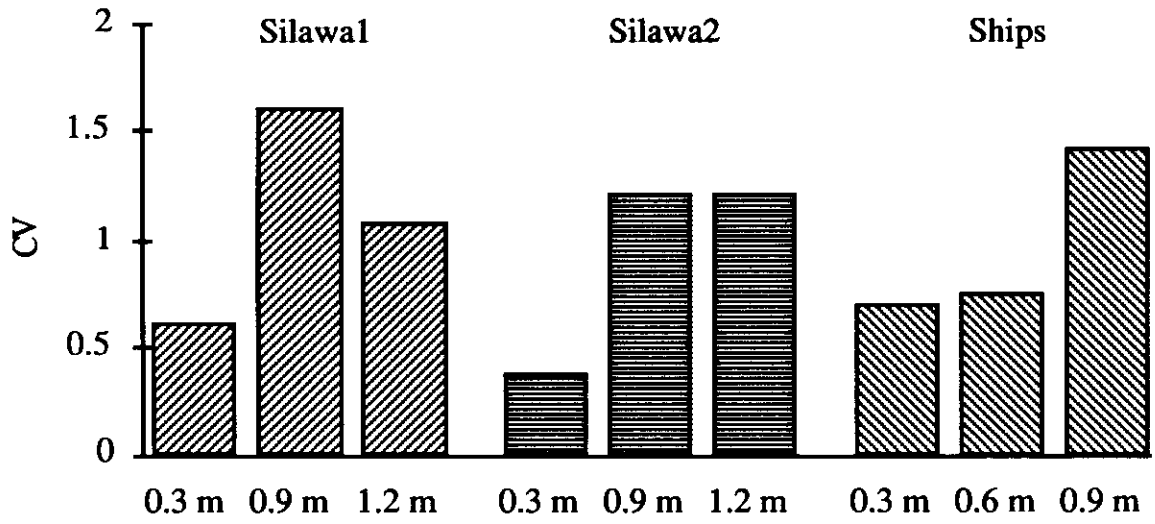

Figure 5. Coefficients of variation of water fluxes at all measured locations.

The bromide fluxes (only measured in Silawa) were highly correlated with the water fluxes, as was expected, and the coefficient of variation of bromide fluxes was very similar to the CV of water fluxes (Fig. 6). The

correlation tended to be higher with increased variability, and therefore depth (Table 1).

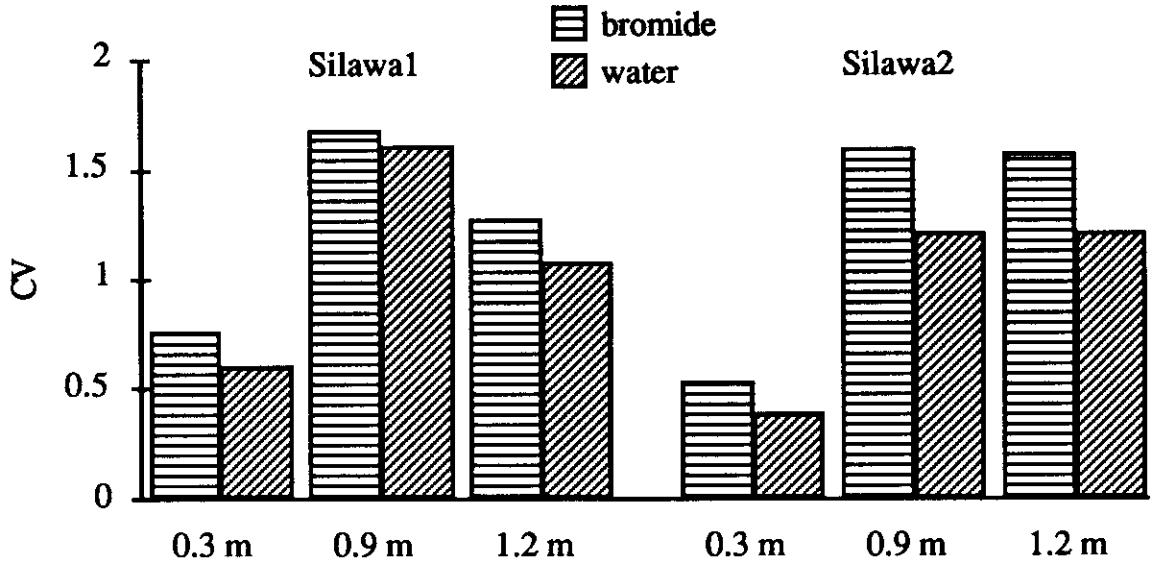

Figure 6. Coefficients of variation of water and bromide fluxes in Silawa.

Silawa1		Silawa2	
depth (m)	correlation coefficient	depth (m)	correlation coefficient
0.3	0.76	0.3	0.82
0.9	0.95	0.9	0.96
1.2	0.85	1.2	0.96

Table 1. Correlation coefficients of water and bromide fluxes in Silawa.

Spatial distribution of relative water fluxes for the Ships clay (Figs. 7 through 9) and Silawa loamy fine sand (Figs. 10 through 15) are displayed. Values higher or less than 1.00 indicate fluxes that are above and below the average flux, respectively. The X coordinate covers 36 cm and the Y coordinate covers 18 cm.

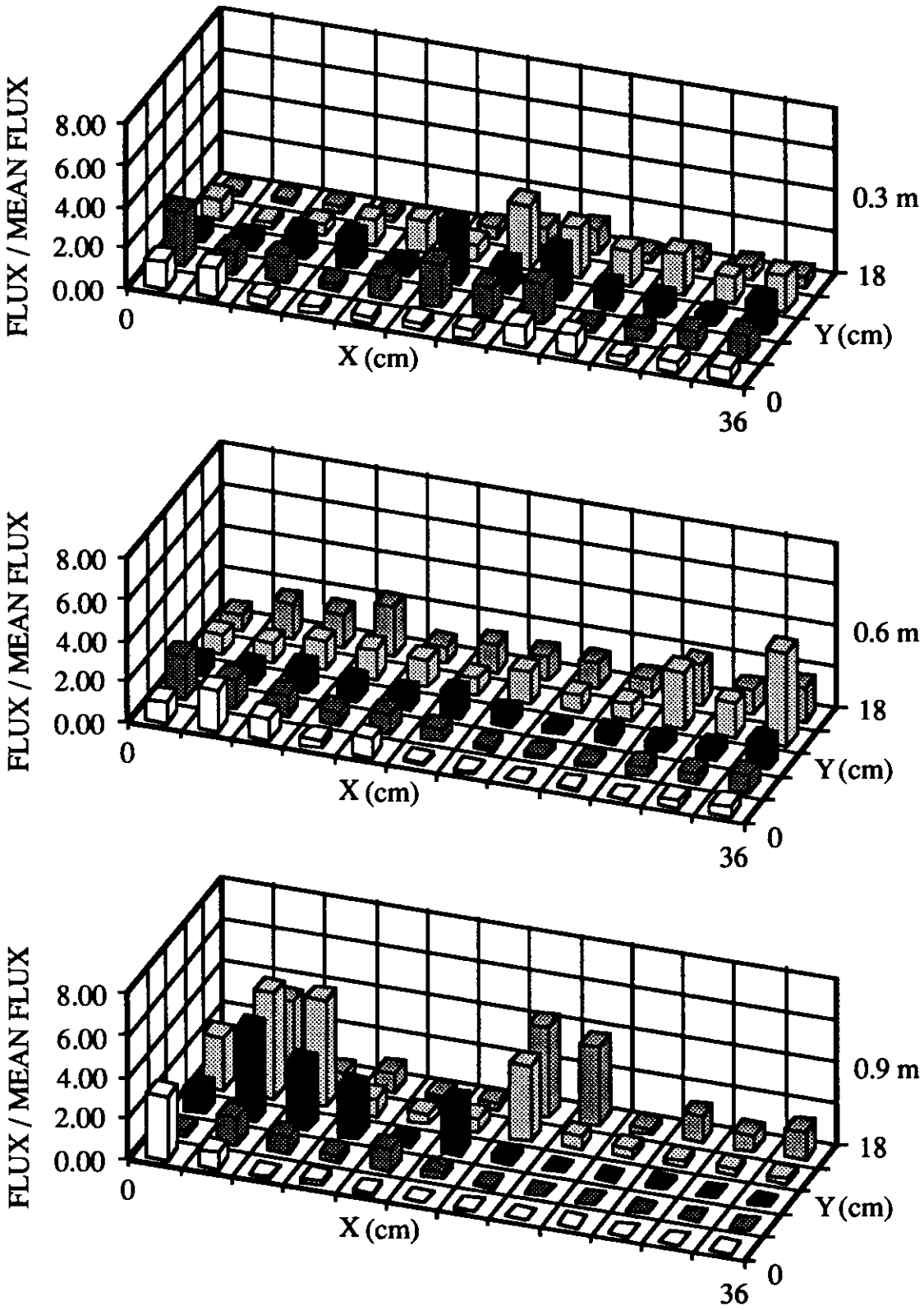

Figure 7. Spatial distribution of relative fluxes in Ships.

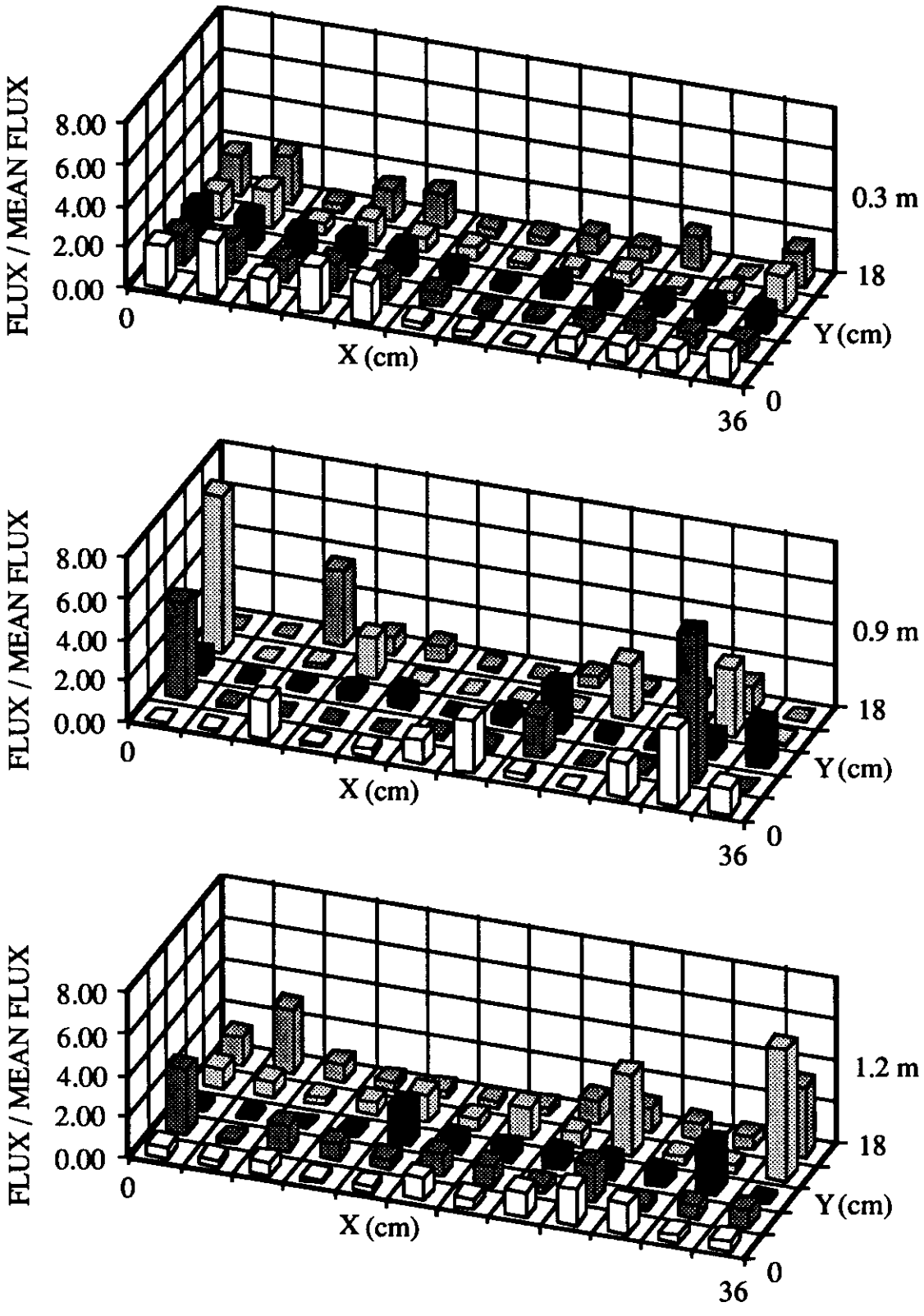

Figure 8. Spatial distribution of relative fluxes in Silawal.

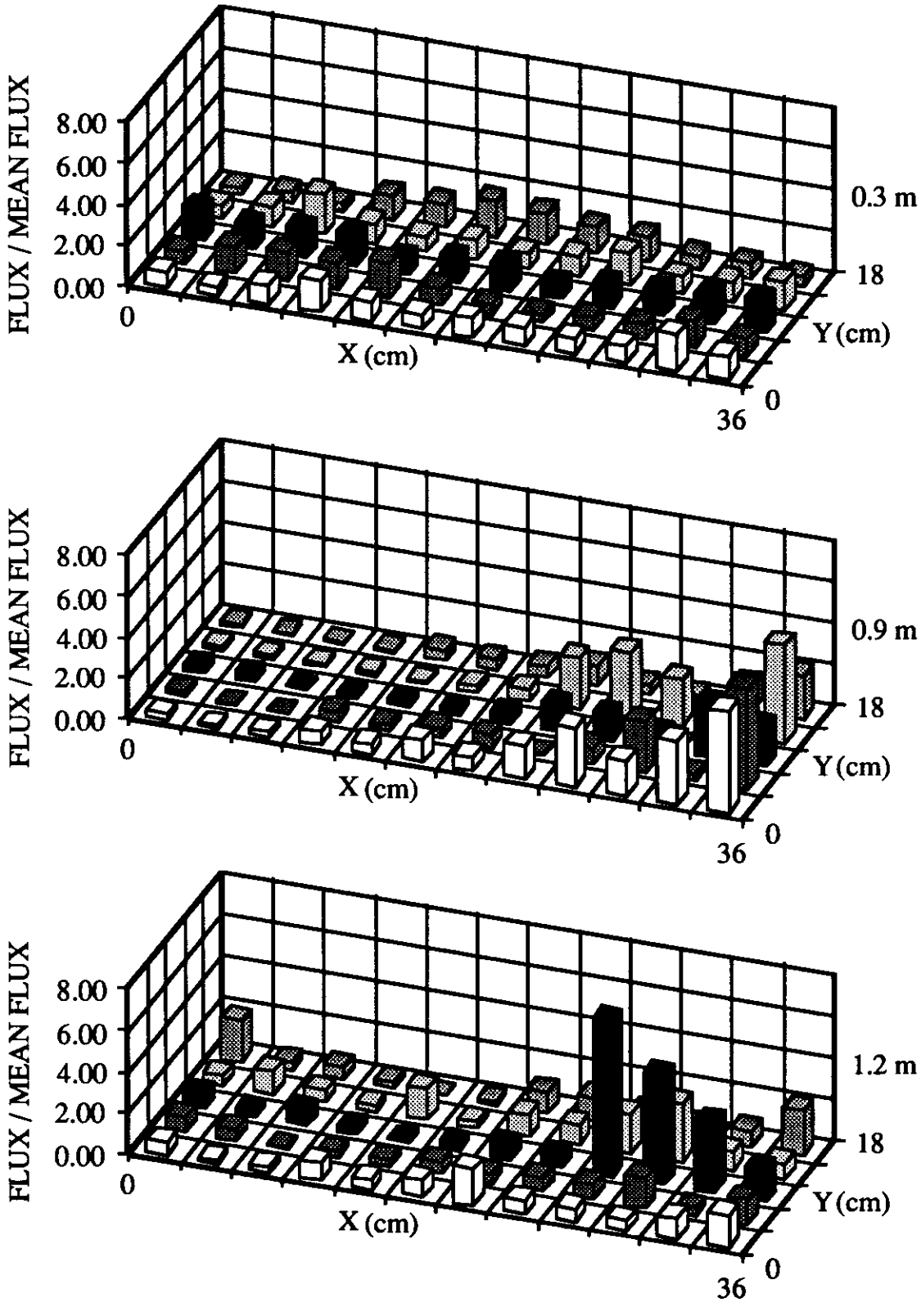

Figure 9. Spatial distribution of relative fluxes in Silawa2.

It can be seen from the frequency distributions of the relative water fluxes that flow paths in Ships clay converged with depth (Fig. 10), i.e. water flowed through a smaller fraction of the cross-sectional area at 0.9 m compared to 0.3 and 0.6 m. This suggests that structural features in the Ships horizons, such as slickensides and blocky structure of different dimensions, can lead to channelization and increased water velocities. In Silawa1, flow convergence from 0.3 to 0.9 m was also found. From 0.9 to 1.2 m, however, divergence occurred, although at 1.2 m it was still converged with respect to 0.3 m (Fig. 11). The same holds for Silawa 2 (Fig. 12). In all cases, frequency distributions of relative intercepted fluxes were positively skewed and resembled a log-normal distribution.

The differences in frequency distributions of the relative fluxes were expected on the basis of morphological features (see the Appendix for profile descriptions). At 0.9 m in Silawa1 and Silawa2 there were many clay films (argillans) around peds while at 0.3 and 1.2 m the soil was more homogeneous. The soil changed from a moderate medium prismatic structure to a weak medium prismatic structure over this distance. Clay films are expected to have low permeability, so that channeling or preferential flow around peds would lead to water flow through a smaller fraction of the cross sectional area than in a homogeneous layer where the whole matrix participates in flow. At 0.9 m in Ships the soil had coarse or very coarse wedge shaped aggregates while at 0.3 and 0.6 m it had a moderate coarse and moderate fine structure, respectively. This change in structure probably causes water to flow through interaggregate pores that are spaced further apart and may cause divergence.

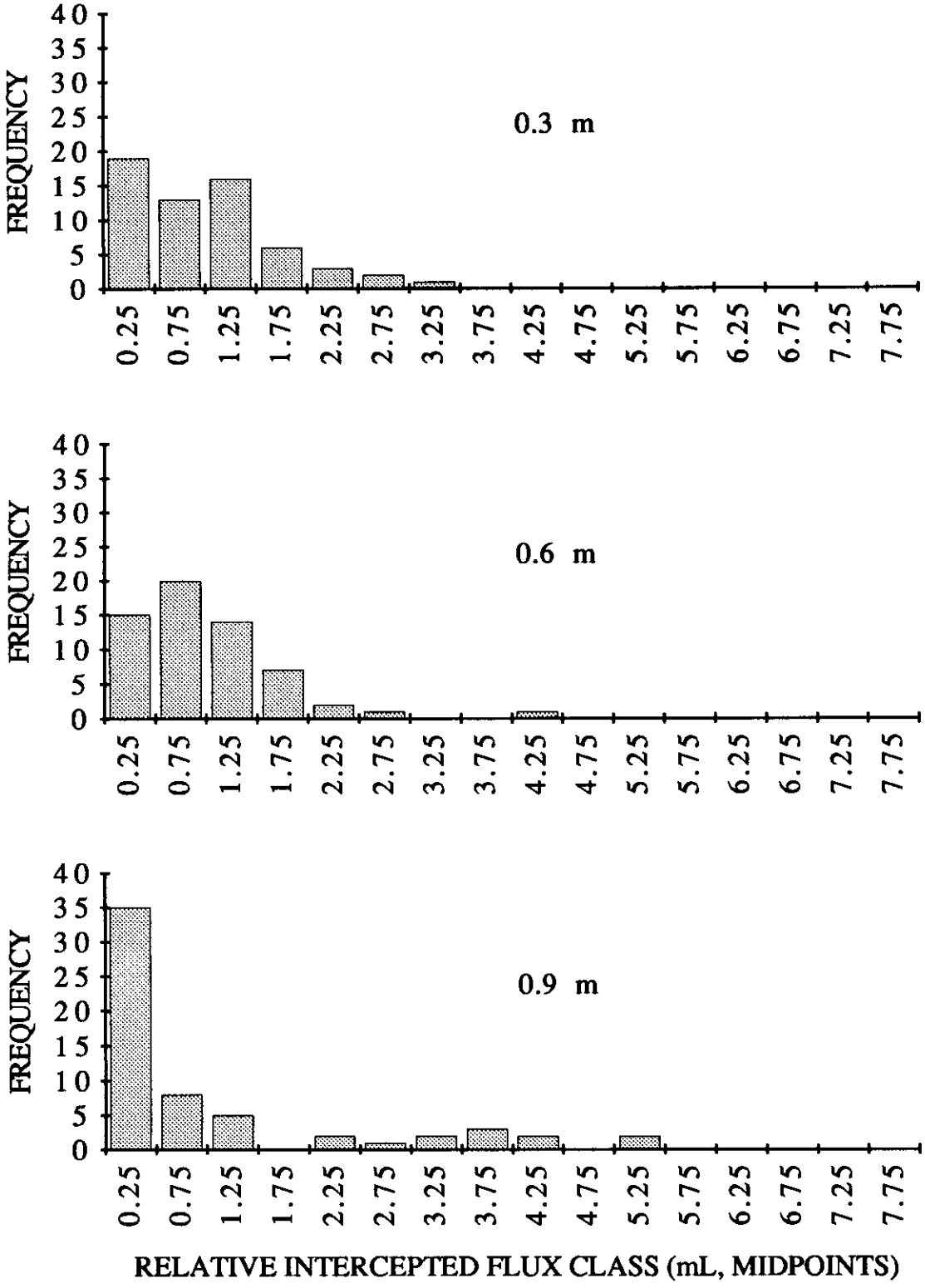

Figure 10. Frequency distribution of relative fluxes in Ships.

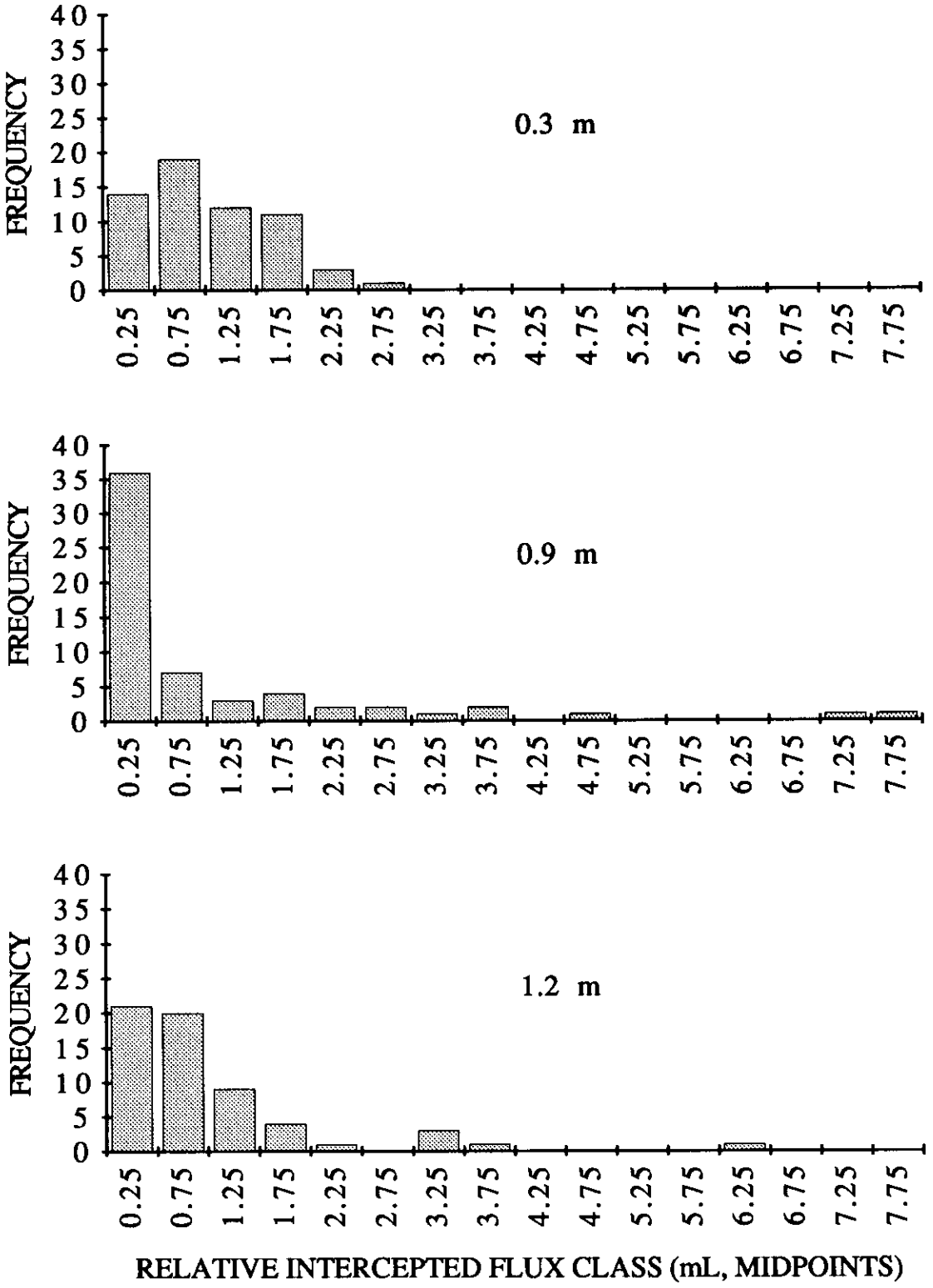

Figure 11. Frequency distribution of relative fluxes in Silawal.

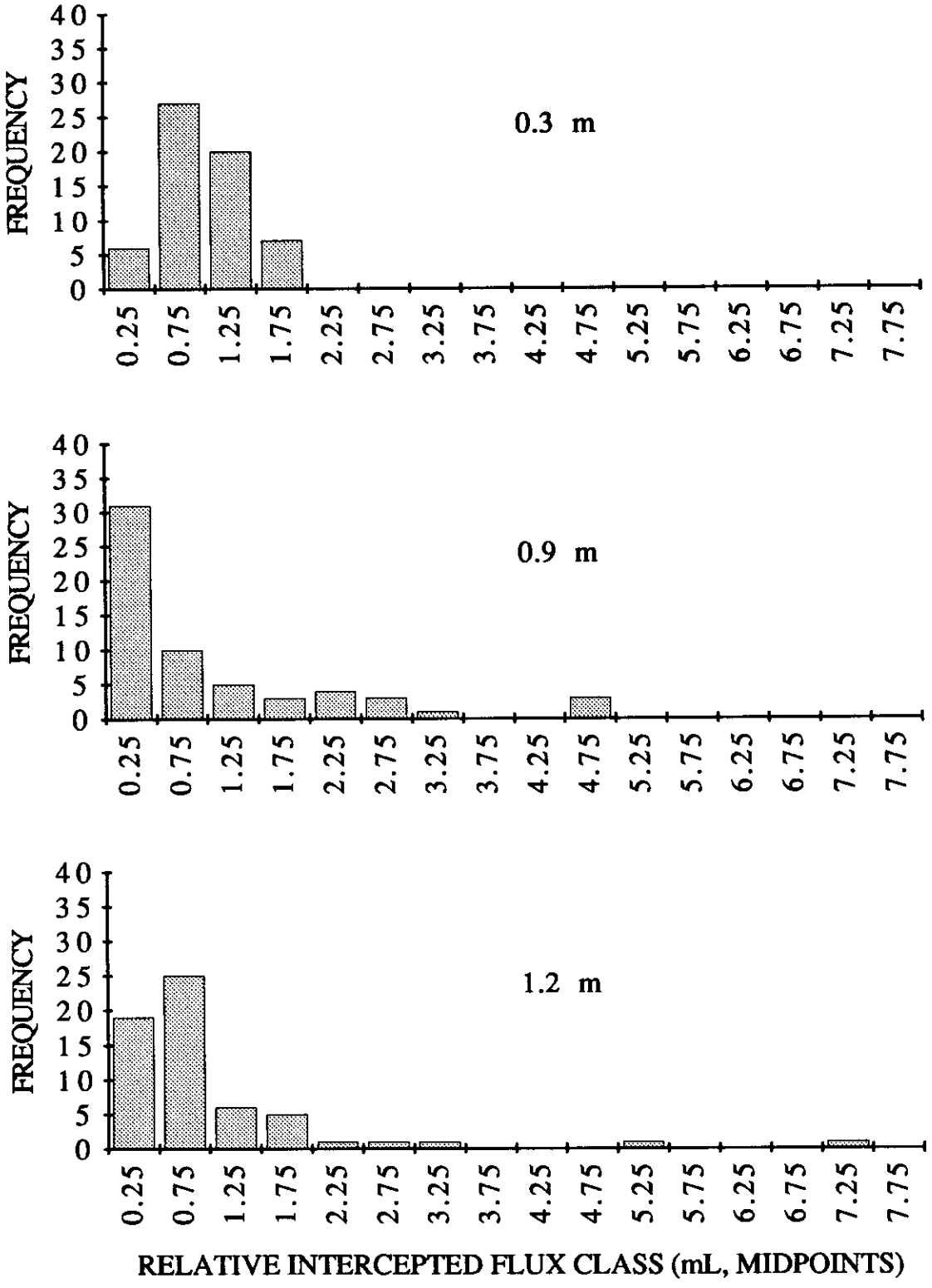

Figure 12. Frequency distribution of relative fluxes in Silawa2.

The (spatial) empirical cumulative and density distributions of the log-transformed water fluxes were calculated as described before, and the cumulative distributions were fitted with a normal distribution (Figs. 13 through 15). The raw sample mean and standard deviation of the data were used for the normal distribution, so no optimization was performed, but this does not influence the correlation coefficient (by definition). The correlation between the empirical and theoretical cumulative distribution is a measure of the likelihood that the data truly have a normal distribution (Table 2). Critical values for the correlation coefficients (c_α) are listed by Ryan *et al.* (1976). They represent the value below which the hypothesis that the data are normally distributed is rejected with an α level of significance. In case of 60 data points, $c_{0.10}$ equals 0.9835, $c_{0.05}$ equals 0.9799 and $c_{0.01}$ equals 0.9710. Since the correlation coefficient is heavily influenced by outliers, and in this project the outliers tended to be the lowest fluxes, the correlation coefficients of the data minus the five lowest values (55 data) were also calculated (Table 2).

Ships			Silawa1			Silawa2		
depth	corr. coeff.		depth	corr. coeff.		depth	corr. coeff.	
(m)	60 data	55 data	(m)	60 data	55 data	(m)	60 data	55 data
0.3	0.9911	0.9892	0.3	0.8801	0.9775	0.3	0.9860	0.9862
0.6	0.9293	0.9661	0.9	0.9701	0.9844	0.9	0.9905	0.9934
0.9	0.9589	0.9583	1.2	0.9754	0.9949	1.2	0.9502	0.9866

Table 2. Correlation coefficients of normal vs log-transformed flux distribution.

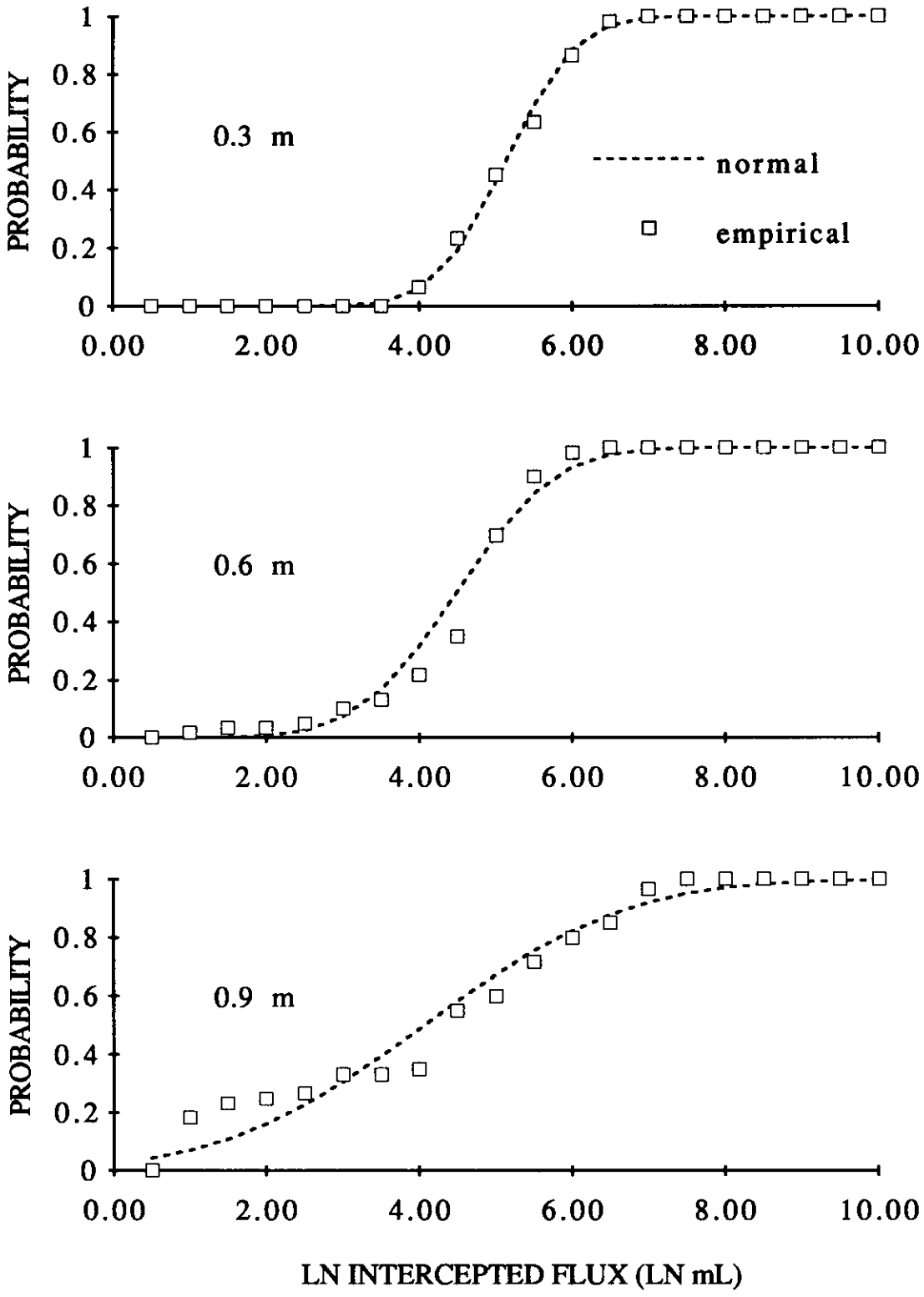

Figure 13. Cumulative distribution of log-transformed fluxes in Ships.

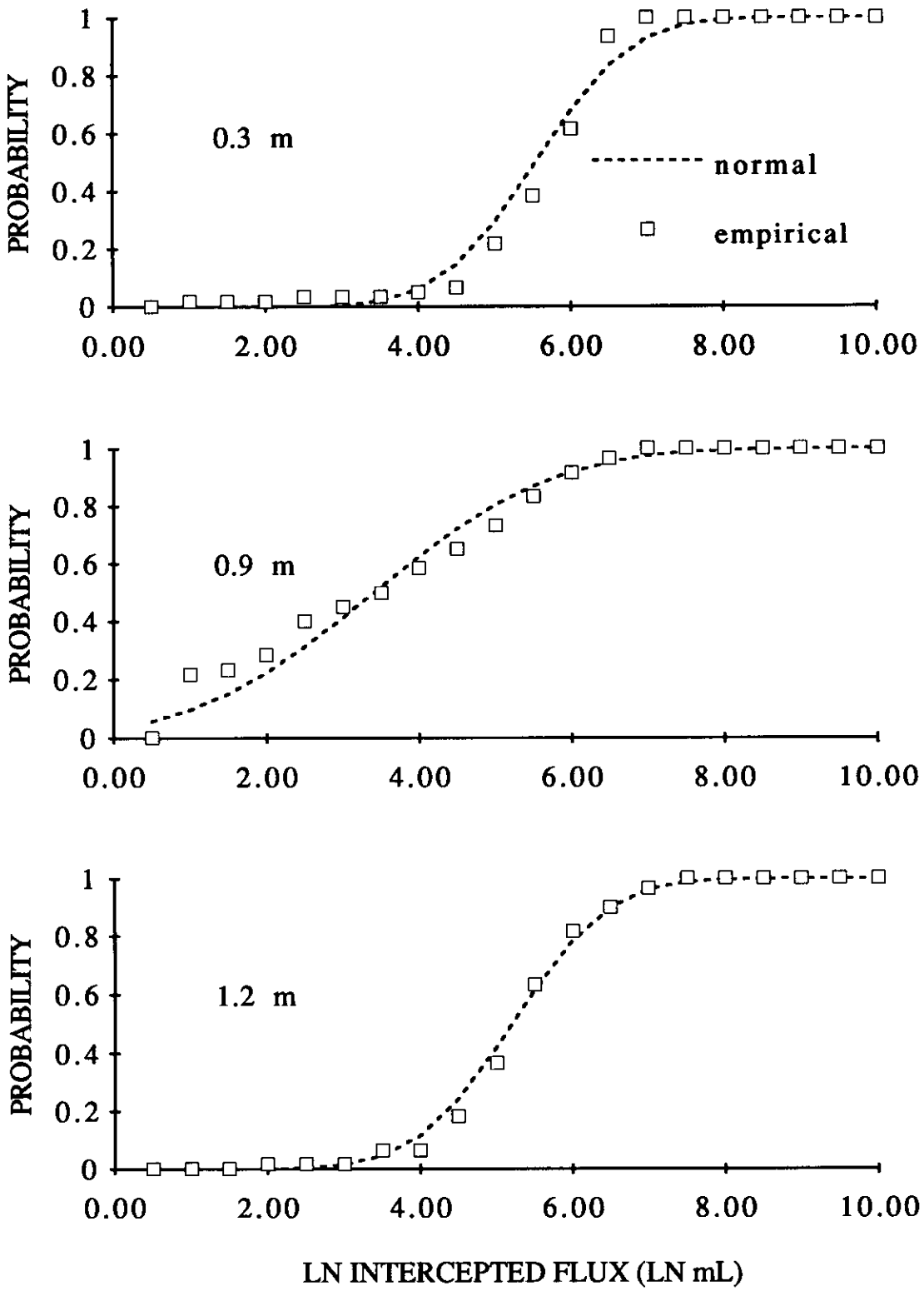

Figure 14. Cumulative distribution of log-transformed fluxes in Silawal.

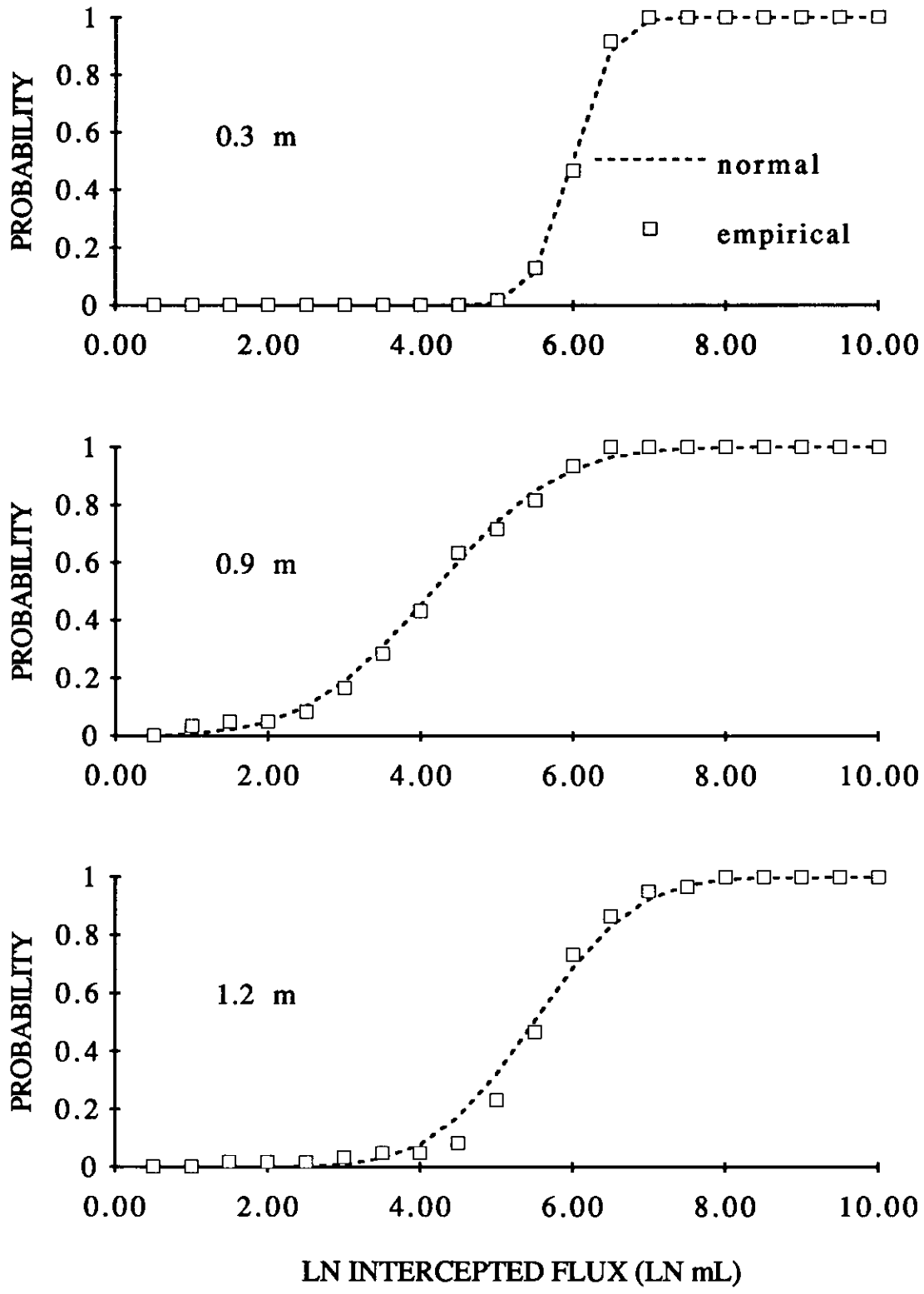

Figure 15. Cumulative distribution of log-transformed fluxes in Silawa2.

From Table 2 it can be seen that the normal hypothesis can not be rejected at a 0.01 level of significance for six of the nine locations using all 60 data and for seven out of nine for the data minus the five lowest values (55 data). This log-normal behavior is also clearly shown in Figs. 13 through 15.

The correlation between the peak bromide concentrations and the intercepted volumes of water flux was very low, and practically all interceptor cells registered the peak concentration in the same measurement time interval. Some of the cells collecting lower fluxes showed higher concentrations than some of the cells collecting higher fluxes, which is probably due to the relatively large sample sizes of intercepted flow. Harvey (1993) found an almost perfect correlation between pore size and bromide concentration in several flooding experiments.

Travel times

The temporal empirical cumulative and density distributions of log-transformed travel "times" ("travel drainage") were calculated as described before, and the cumulative distributions were fitted with a normal distribution. The optimization of the model parameters μ and σ was done by fitting the normal-empirical curve to a straight 45^{o} line. The retransformed travel time distributions are shown in Figs. 16 through 19 and the correlation coefficients of the empirical and theoretical cumulative distribution are listed in Table 3.

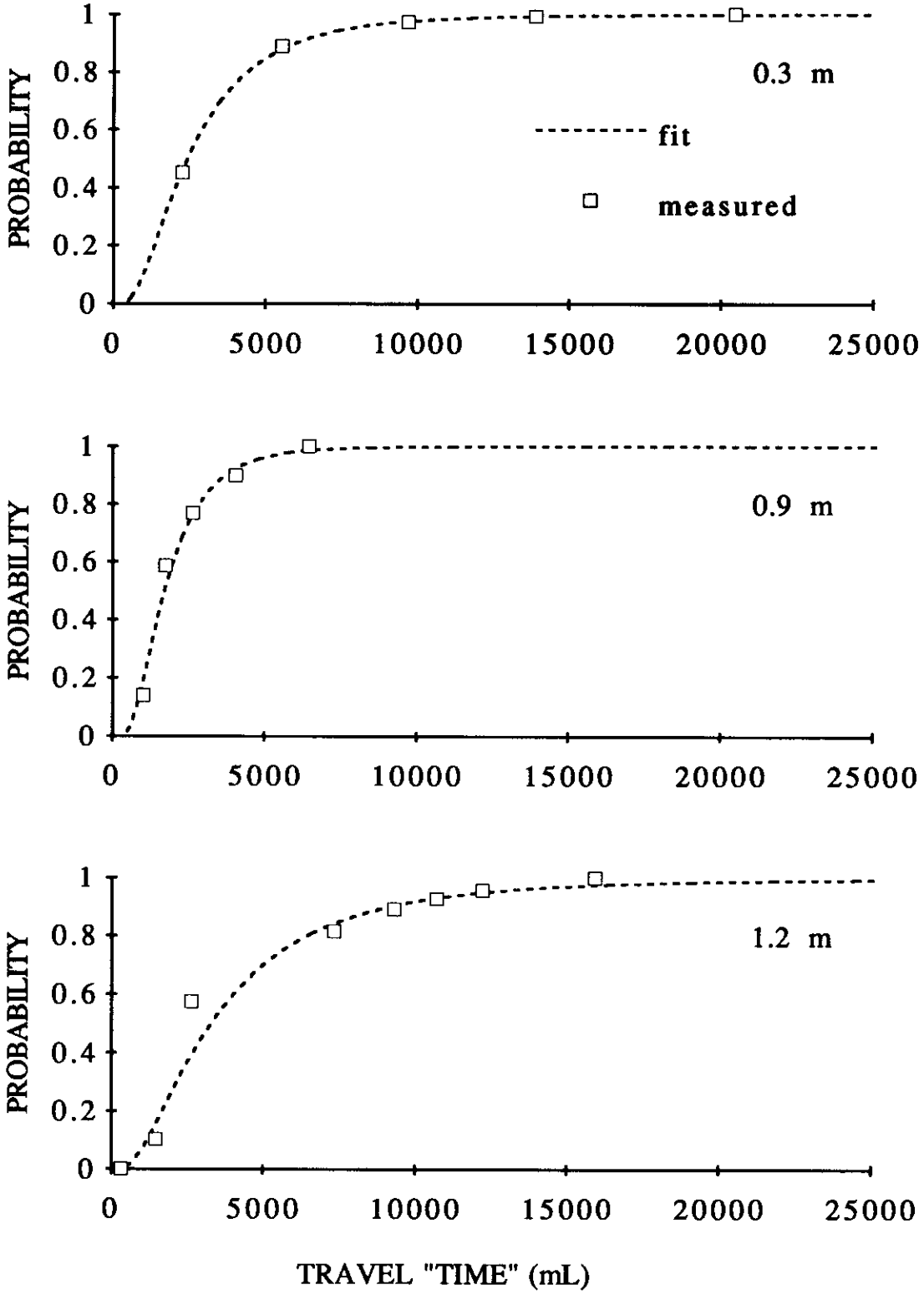

Figure 16. Cumulative distribution of travel times in Silawal.

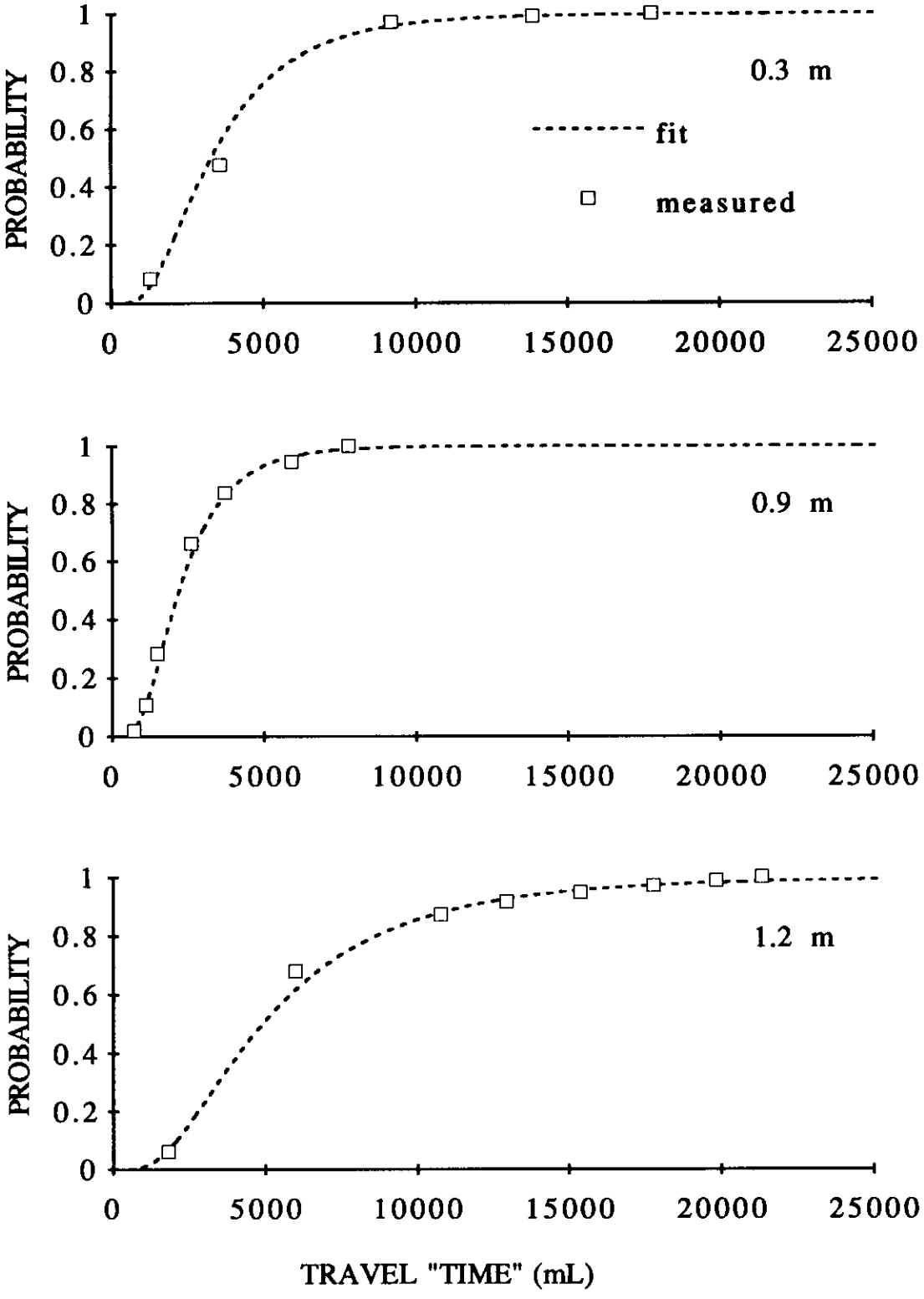

Figure 17. Cumulative distribution of travel times in Silawa2.

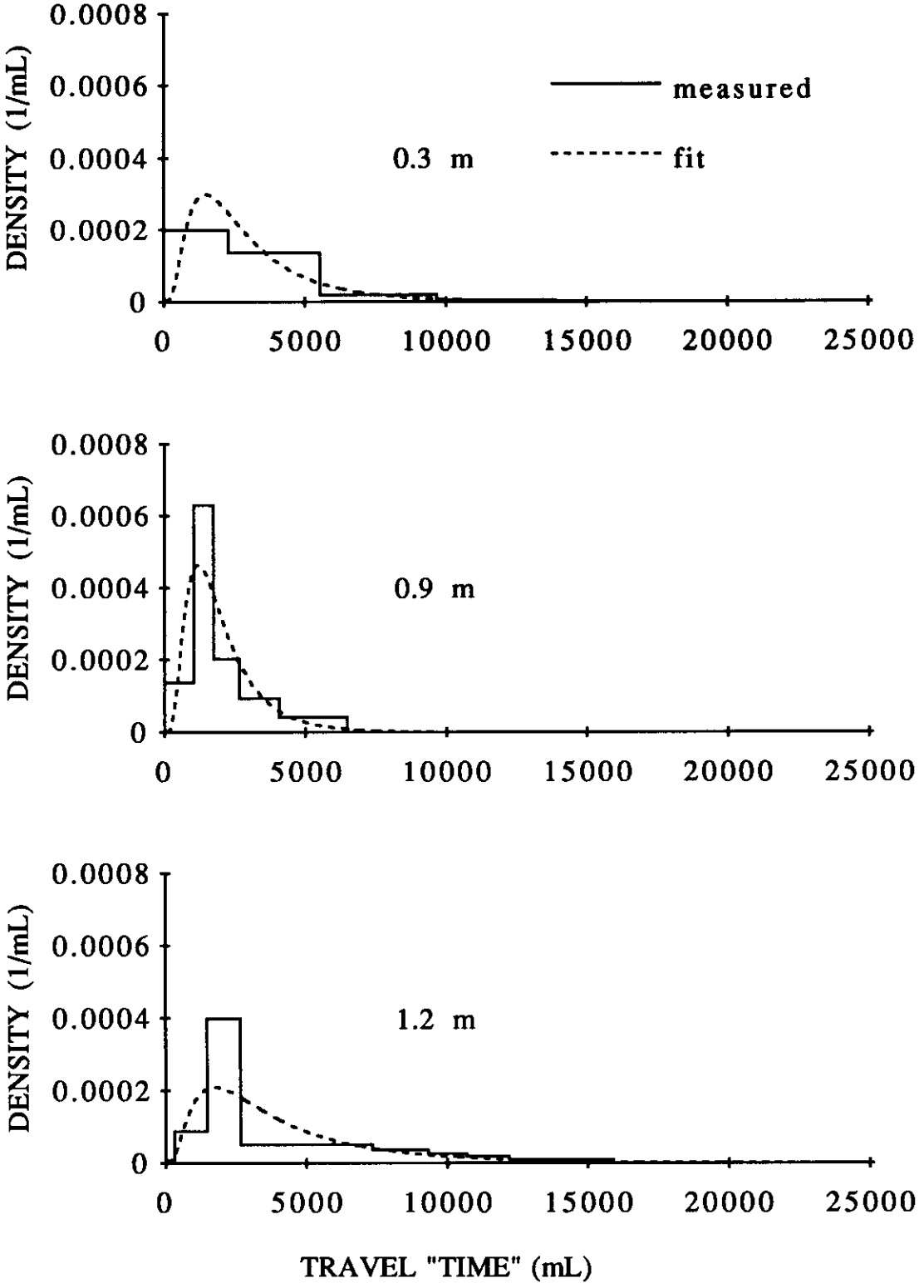

Figure 18. Probability density distribution of travel times in Silawal.

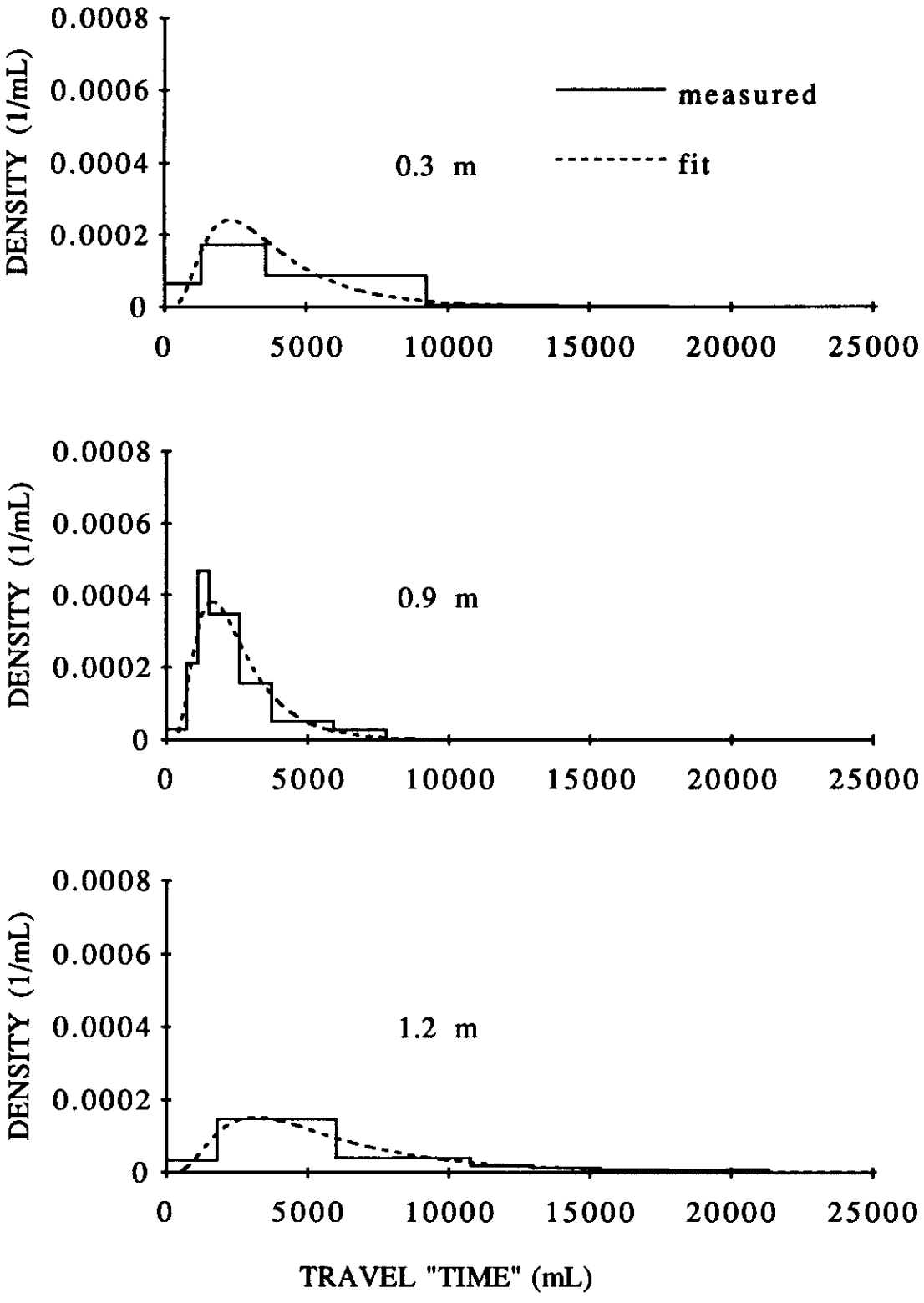

Figure 19. Probability density distribution of travel times in Silawa2.

Silawa1		Silawa2	
depth (m)	correlation coefficient	depth (m)	correlation coefficient
0.3	0.9993	0.3	0.9951
0.9	0.9824	0.9	0.9973
1.2	0.9911	1.2	0.9969

Table 3. Correlation coefficients of normal vs log-transformed travel time cumulative distribution.

The log-transformed travel "times" show nearly perfect log-normal behavior as can be seen from Table 3 and Figs. 16 through 19. The hypothesis that the travel times are log-normally distributed can not be rejected even at a 0.10 level of significance.

Travel time pdd's at 0.9 m depth were predicted from 0.3 m and at 1.2 m from 0.3 and 0.9 m depth (Figs. 20 and 21), using the stochastic-convective log-normal transfer function model as described earlier. The curves at 1.2 m predicted from 0.9 m were close to the actual measurements. The curves at 0.9 and 1.2 m predicted from 0.3 m, however, differed considerably from the actual measurements. This might be due to the fact that the 0.3 m measurements were taken in the lab, changes in soil structure, imperfect boundary conditions, or because the flux was intercepted over a small area. If it is due to changes in soil structure, then water flux measurements at the surface may not be suitable for making travel time predictions.

The transfer function model used here assumes a constant profile in which the travel time pdd's are the same for layers with the same thickness. In reality, the Silawa loamy fine sand, like most soils, has layers

with different flow properties. However, for depths close to the calibration depth only a small prediction error associated with the assumption of a constant profile would be expected. Changes in soil structure, which are more likely with increased distance between predicted and calibrated depth, increase prediction errors as shown in this study. The model can be adjusted for layered soils by using separate pdf's for every horizon. This makes it more complicated and takes more computer time, but might increase the accuracy of the model dramatically. What occurs at greater depths was not measured and is therefore uncertain. It is expected that deviations from the existing model predictions will increase.

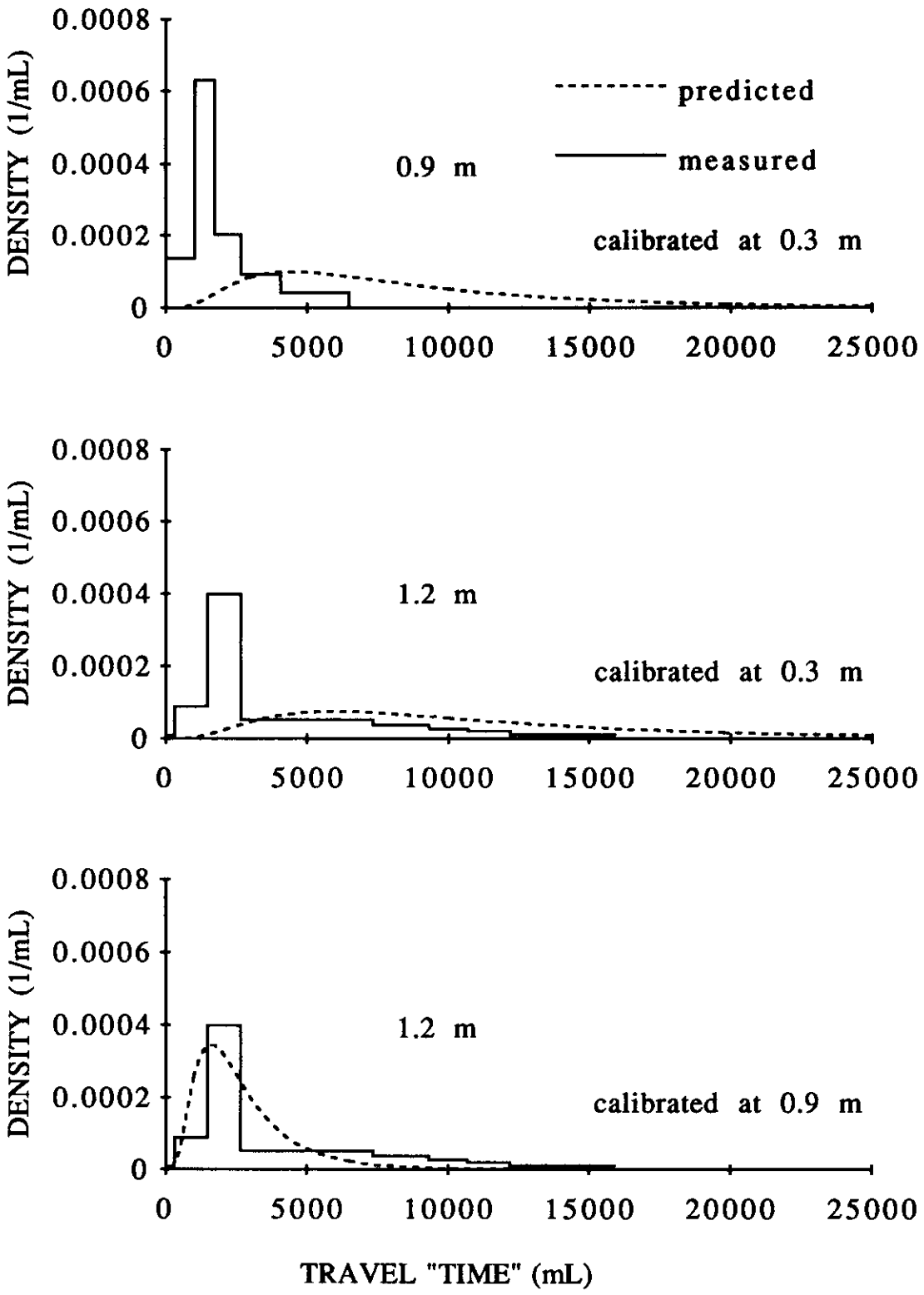

Figure 20. Travel time predictions in Silawa1.

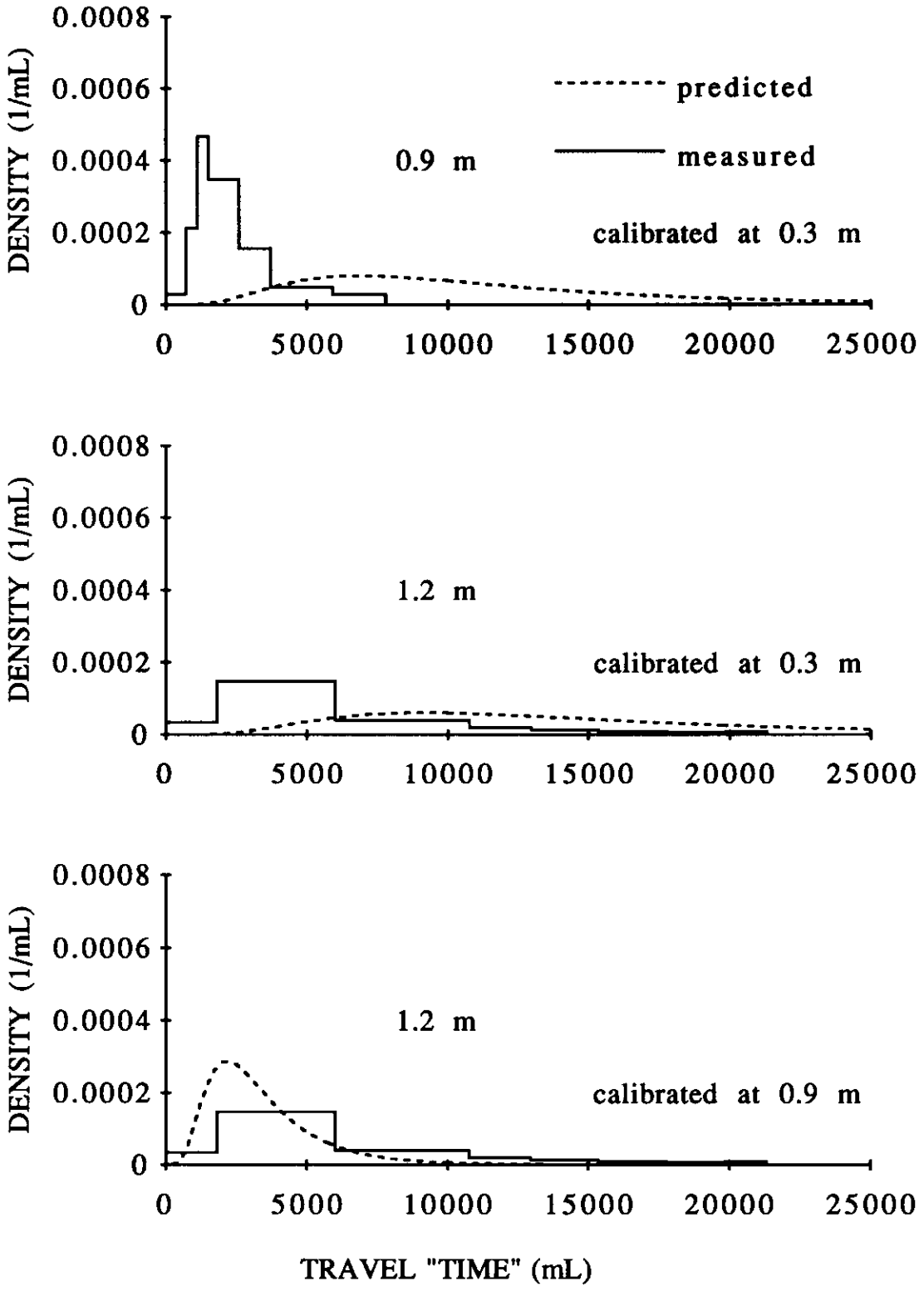

Figure 21. Travel time predictions in Silawa2.

CONCLUSIONS AND RECOMMENDATIONS

The goal of this experimental project was to find relationships between water fluxes, solute travel times and soil structure. The equipment and procedures developed for this study seem to be well-suited for this purpose. The multiple flow interceptor method favors the analysis of variability of fluxes, while the determination of the travel time probability distribution by using the flow interceptor may be less accurate than conventional methods. It is beneficial to have many measurements of concentration with time to estimate the travel time pdd's. The reason for the loss of accuracy with the flow interceptor is that small samples of intercepted fluxes are difficult to analyze for bromide and are more susceptible to contamination during the measuring process and analysis. If the samples of all 60 interceptors were combined (mixed) for the bromide analysis, then more measurements could be conducted in time and a more accurate breakthrough curve and travel time pdd could be constructed.

The water fluxes and bromide fluxes showed very high correlation, as might be expected, but water fluxes and travel time were not well correlated. This is likely due to to the fact that not enough samples could be taken for more accurate calculations of the travel time pdd's. Also, spatial flux distributions were found to be related to soil structure. The coefficients of variation of the water and bromide fluxes were lowest for the sandy top horizon of Silawa and highest at 0.9 m in both Silawa and Ships. This stresses the importance of a better understanding of water and solute fluxes and soil structure relationships. Continued study on this subject, using non-conservative tracers, might reveal interesting results.

Water flux measurements at the surface alone were insufficient for predicting water and solute flow at lower depths. More research on soil structure and water flow relationships is necessary for more accurate contaminant flow models and predictions based on existing datasets.

The log-normal transfer function approach seems well-suited for structured soils and can be made more accurate by using different travel time pdf's for different layers. The log-normal distribution is convenient and seemed to fit the data well.

The convergence of water flow with depth measured in Ships clay (in its physical condition as observed during the experiments in the fall of 1992) exceeded that measured in Silawa loamy fine sand (in the fall of 1993). Bypass flow in Ships clay and Silawa loamy fine sand can transport pollutants quickly through a small portion of the soil profile. Since sorption and degradation rates decrease with increasing water flow rates, chemicals in macropores may move through the rootzone faster than expected by traditional theory. We are presently studying the physical and chemical properties of these flow paths.

APPENDIX

Ships profile description

SOIL SERIES: Ships

SOIL CLASSIFICATION: very-fine, mixed, thermic, Chromic Udic Haplusterts

LOCATION: Texas A & M University farm in Burleson County, about 0.5 mile south of Highway 60 about 0.25 mile west of Brazos River

PARENT MATERIAL: Clayey alluvial sediments

VEGETATION: Bermudagrass pasture

TOPOGRAPHY: Nearly level flood plain

SOIL DESCRIPTION (colors for moist soils unless stated)

A_p1 0 to 10 cm; dark reddish brown (5YR3/4) clay, reddish brown (5YR 4/3) dry; dry; weak coarse platy parting to moderate very fine angular blocky structure in the upper 1 cm, moderate very fine angular and subangular blocky structure in the lower 9 cm; very sticky, firm, very hard; many surface crusts, about 1 cm thick, and 2 to 5 cm wide & long with medium inter-crust cracks; many fine to coarse intercloddy clusters; common very fine roots; medium to strong effervescent; pH 8; clear smooth boundary.

A_p2 10 to 27 cm; dark reddish brown (5YR 3/4) clay; strong very coarse angular blocky parting to moderate very thick platy structure; extremely hard; common very coarse interpedal cracks; common very fine and few medium roots; slightly to strongly effervescent; pH 8; clear smooth boundary.

$B_{ss}1$ 27 to 42 cm; dark reddish brown (5YR 3/4) clay; moderate coarse angular blocky parting to moderate medium angular blocky structure; firm; few very fine spherical intrapedal pores; many slickensides, most 15 to 20 cm across, 45 to 60° angle; many pressure faces; few 2 to 3 mm diameter shells; few 2 to 3 mm diameter carbonate nodules; slightly to strongly effervescent; pH 8; gradual smooth boundary.

$B_{ss}2$ 42 to 70 cm; dark reddish brown (5YR 3/4) clay ; moderate very fine angular blocky structure; firm; few very fine spherical intrapedal pores; many slickensides, most 15 to 20 cm across, 45 to 60° angle; many pressure faces; few 2 to 3 mm diameter shells; few 2 to 3 mm diameter carbonate nodules; slightly to strongly effervescent; pH 8; clear smooth boundary.

$B_{ss}3$ 70 to 122 cm; stratified layers of reddish brown (5YR 4/4) and dark gray (10YR4/1) clay, with some strong brown (7.5YR5/6) mottles; coarse or very coarse wedge-shape blocky aggregates parting to weak to moderate fine and very fine angular blocky structure; firm; few very fine spherical intrapedal pores; many slickensides crossing the bedding planes, most 10 to 15 cm across, 45 to 60° angle; many pressure faces; common 1 to 3 mm diameter carbonate nodules; slightly to strongly effervescent; pH 8; clear smooth boundary.

BC 122 to 132 cm; stratified layers of very dark grayish brown (10YR 3/2) and brown (7.5YR5/4) silty clay loam; weak to moderate fine and very fine angular blocky structure; firm; pH 8; clear smooth boundary.

2C 132 to 170+ cm; yellowish red (5YR 4/6) silt loam; structureless; friable; pH8.

Silawa profile description

SOIL SERIES: Silawa

SOIL CLASSIFICATION: Fine-loamy, siliceous, thermic, Ustic Haplustalfs

LOCATION: Brazos river terrace, Brazos county.

PARENT MATERIAL: Sandy and loamy sediments

VEGETATION: Pasture

TOPOGRAPHY: 3-5% slope

SOIL DESCRIPTION (colors for moist soils unless stated)

A1 0 to 10 cm; brown (10YR 4/3) loamy fine sand; weak fine to medium granular structure; very friable; many medium, fine, and very fine roots; many packing pores; clear smooth boundary.

A2 10 to 25 cm; brown (10YR 4/3) loamy fine sand; weak medium subangular blocky structure; very friable; common medium, fine, and very fine roots; many packing pores; gradual smooth boundary.

E 25 to 34 cm; yellowish brown (10YR 5/4) loamy fine sand; weak medium subangular blocky structure; very friable; common medium, fine and very fine roots; many packing pores; abrupt smooth boundary.

Bt1 34 to 59 cm; yellowish red (5YR 4/6) sandy clay; moderate medium prismatic structure; firm; few medium and common fine and very fine roots; common fine (up to 0.5 mm) rounded within matrix pores, many between ped vertical and horizontal structural pores; thin dark reddish brown (2.5YR 3/4) argillans; clear smooth boundary.

Bt2 59 to 103 cm; red (10R 4/8) sandy clay; moderate medium prismatic structure; firm; few medium and common fine and very fine roots; common fine (up to 0.5 mm) rounded within matrix pores, many between ped vertical and horizontal structural pores; thick reddish brown (5YR 4/4) argillans and very thick yellowish brown (10YR 5/6) hematite depleted neocutans around peds; clear smooth boundary.

Bt3 103 to 129 cm; red (2.5YR 4/8) sandy clay loam; weak medium prismatic parting to weak medium subangular blocky structure; friable; few medium, fine, and very fine roots; few fine (up to 1 mm) rounded within matrix pores, common vertical and few horizontal structural pores; thin discontinuous dark reddish brown (2/5YR 3/3) argillans; gradual smooth boundary.

BCt 129 to 135+ cm; yellowish red (5YR 5/8) fine sandy loam; weak medium subangular blocky structure; friable; few fine roots; few fine (up to 1 mm) rounded within matrix pores, few structural pores.

Throughout the profile there are few biopores with fecal pellets (probably from fire ants) up to 1 cm in size. There are also 1 to 3 percent rounded siliceous pebbles and/or gravel throughout.

REFERENCES

J. Bouma. 1984. Using soil morphology to develop measurement methods and simulation techniques for water movement in heavy clay soil. In Water and solute movement in heavy clay soils. Proc. of an ISSS Symposium. Edited by J. Bouma and P.A.C. Raats. ILRI publication No. 37, Wageningen, The Netherlands.

V.T. Chow. 1964. Runoff. In Handbook of applied hydrology. McGraw-Hill Book Company.

G.M. Coen and G. Wang. Estimating vertical saturated hydraulic conductivity from soil morphology in Alberta. Can. J. Soil Sci. 69:1-16.

K. Economy and R.S. Bowman. 1992. Preferential flow effects on chemical transport and retardation in soils. New Mexico Water Resources Research Institute WRRI Report No. 272:90-91.

J.W. Harvey. 1993. Measurement of variation in soil solute tracer concentration across a range of effective pore sizes. Water. Resour. Res. 29:1831-1837.

W.A. Jury and H. Flühler. 1992. Transport of chemicals through soil: mechanisms, models and field applications. Adv. Agr. 47:141-201.

W.A. Jury and K. Roth. 1990. The solute transfer function for transport through soil. In Transfer functions and solute movement through soil: theory and applications. Birkhäuser Verlag, Basel, Germany. 226pp.

D.R. Nielsen, J.W. Biggar and K.T. Erh. 1973. Spatial variability of field-measured soil-water properties. Hilgardia 42:215-259.

T.A. Ryan, B.L. Joiner and B.F. Ryan. 1976. Table A.14. In Minitab II reference manual. 100pp.

J.S. Shepard. 1993. Using a fractal model to compute the hydraulic conductivity function. Soil Sc. Soc. Am. J. 57:300-306.

R.E. White. 1987. A transfer function model for the prediction of nitrate leaching under field conditions. J. Hydrol. 92:207-222.